Title

Integral bHLH factor regulation of cell cycle exit and RGC differentiation

Journal

Developmental Dynamics, 247(8)

ISSN

1058-8388

Authors

Maurer, Kate A
Kowalchuk, Angelica
Shoja-Taheri, Farnaz
et al.

Publication Date

2018-08-01

DOI

10.1002/dvdy.24638

Peer reviewed

HHS Public Access

Author manuscript

Dev Dyn. Author manuscript; available in PMC 2019 August 01.

Published in final edited form as:

Dev Dyn. 2018 August ; 247(8): 965–975. doi:10.1002/dvdy.24638.

Integral bHLH factor regulation of cell cycle exit and RGC differentiation

Kate A. Maurer[1,*,#], **Angelica Kowalchuk**[2,*], **Farnaz Shoja-Taheri**[2,&], and **Nadean L. Brown**[1,2]

[1]Division of Developmental Biology, Cincinnati Children's Hospital Research Foundation, Cincinnati, OH, 45229

[2]Department of Cell Biology and Human Anatomy, University of California Davis, School of Medicine, Davis, CA 95616

Abstract

Background—In the developing mouse embryo, the bHLH transcription factor *Neurog2* is transiently expressed by retinal progenitor cells and required for the initial wave of neurogenesis. Remarkably, another bHLH factor, *Ascl1*, normally not present in the embryonic *Neurog2* retinal lineage, can rescue the temporal phenotypes of *Neurog2* mutants.

Results—Here we show that *Neurog2* simultaneously promotes terminal cell cycle exit and retinal ganglion cell differentiation, using mitotic window labeling and integrating these results with retinal marker quantifications. We also analyzed the transcriptomes of E12.5 GFP-expressing cells from *Neurog2*$^{GFP/+}$, *Neurog2*$^{GFP/GFP}$, and *Neurog2*$^{Ascl1KI/GFP}$ eyes, and validated the most significantly affected genes using qPCR assays.

Conclusions—Our data support the hypothesis that *Neurog2* acts at the top of a retinal bHLH transcription factor hierarchy. The combined expression levels of these downstream factors are sufficiently induced by ectopic *Ascl1* to restore RGC genesis, highlighting the robustness of this gene network during retinal ganglion cell neurogenesis.

Keywords

Neurog2; Atoh7; Ascl; retinal ganglion cell; neurogenesis; bHLH

Introduction

In the vertebrate retina, seven neuronal and glial cell classes arise from a common pool of retinal progenitor cells (RPCs), in a highly ordered and partially overlapping sequence (Young, 1985; Turner and Cepko, 1987; Turner et al., 1990; Rapaport et al., 2004). The RPC population expands through continuous rounds of mitotic cell division, which must be integrated with tissue morphogenesis and cell fate determination. The timing of the terminal

Corresponding Author: Nadean L. Brown, Department of Cell Biology and Human Anatomy, University of California, Davis, Room 4407A Tupper Hall, Davis, CA 95616, nlbrown@ucdavis.edu, Voice: 530-752-7806.

*These authors made equal contributions

#Present address: Medpace Central Laboratories Cincinnati, OH 45229

&Present address: Department of Biomedical Engineering Emory University, Atlanta, GA

S-phase (or birthdate) of an RPC strongly influences its postmitotic identity. Retinal neurogenesis initiates centrally and expands outwards towards the periphery (Prada et al., 1991; Hu and Easter, 1999; McCabe et al., 1999). In mice, the first wave of neurogenesis begins on embryonic day (E)11.0 and is complete by E13.5 (Sidman, 1961; Hufnagel et al., 2010). Since retinal ganglion cells (RGCs) are the first cell class to differentiate in all vertebrate eyes, their formation is synonymous with the initial wave of neurogenesis.

The onset of ganglion cell formation is characterized by activation of the basic helix-loop-helix (bHLH) transcription factor *Atoh7*, in newly postmitotic RPCs. Although *Atoh7*-expressing cells give rise to all seven major cell classes (Feng et al., 2010; Brzezinski et al., 2012), *Atoh7* bestows competence to a subset of these cells to develop as RGC neurons. The complete absence of RGCs and optic nerves in *Atoh7* mutant mice illustrates its importance (Brown et al., 2001; Wang et al., 2001). However, downstream of *Atoh7*, the transcription factors *Pou4f2* and *Isl1* are essential to lock-in the RGC differentiation program (Mu et al., 2008; Pan et al., 2008; Li et al., 2014; Wu et al., 2015). In the absence of either gene, RGCs are specified, but subsequently undergo significant apoptosis (65-80%) prior to birth (Gan et al., 1996; Gan et al., 1999; Mu et al., 2008; Pan et al., 2008). *Pou4f2* and *Isl1* double mutant retinas have an even greater loss of RGCs (>95%), highlighting their synergistic relationship (Pan et al., 2008; Li et al., 2014; Wu et al., 2015). *Pou4f1, Myt1*, *Ebf3, Onecut1* and *Onecut2* either act in parallel or downstream of *Pou4f2* and *Isl1* during RGC genesis (Erkman et al., 1996; Mu et al., 2008; Jin et al., 2010; Wu et al., 2012; Shi et al., 2013; Gao et al., 2014). However, a better understanding of the regulatory relationships among these genes is still lacking.

Other bHLH proneural factors are also active during retinogenesis. Indeed, *Neurog2* initiates retinal expression in mice at E11.0, within a subset of mitotic RPCs, including those at the leading edge of neurogenesis (Yan et al., 2001; Ma and Wang, 2006; Hufnagel et al., 2010; Brzezinski et al., 2011). In these RPCs, *Neurog2* directly activates *Atoh7* transcription through an evolutionarily conserved E-box in the primary *Atoh7* retinal enhancer (Riesenberg et al., 2009; Skowronska-Krawczyk et al., 2009). In the absence of *Neurog2*, *Atoh7* expression is delayed along with the advancement of *Pou4f2*+ RGCs (Hufnagel et al., 2010). Another bHLH factor, *Ascl1*, is also expressed by a cohort of proliferating RPCs, beginning at E12.5 (Jasoni and Reh, 1996; Brzezinski et al., 2011). Despite partially overlapping expression domains in the prenatal retina, *Neurog2* and *Ascl1* demarcate distinct lineages (Brzezinski et al., 2011). Thus, it was unexpected that misexpression of *Ascl1* in the *Neurog2* lineage rescued *Atoh7* expression and the wave of (RGC) neurogenesis (Hufnagel et al., 2010). One explanation is that *Neurog2* and *Ascl1* are largely expressed by proliferating RPCs thus, share a common set of downstream targets in the retina. (Jasoni and Reh, 1996; Yan et al., 2001; Ma and Wang, 2006). Alternatively, the presence of multiple bHLH factors, which include *Neurod1*, *Neurod4*/*Math3*, and *Olig2*, endow the RGC gene network with sufficient redundancy for the establishment of functional optic nerves. To distinguish among these possibilities, we used transcriptomics and gene expression analyses to identify genes that require Neurog2 for their expression but are also upregulated upon *Ascl1* rescue of RGC development.

Results

Neurog2 regulation of cell cycle exit

We hypothesized that *Neurog2* must normally regulate some aspect of cell cycle exit, because the percentages of both actively mitotic and apoptotic RPCs did not differ among *Neurog2*$^{GFP/+}$ (control), *Neurog2*$^{GFP/GFP}$ (mutant), and *Neurog2*$^{Ascl1KI/GFP}$ (rescue) embryos (Hufnagel et al., 2010). To test this idea, we performed a BrdU window labeling on embryos of all three genotypes (Repka and Adler, 1992). A single injection of BrdU was given intradermally to pregnant dams at either 1.5 or 18 hours prior to sacrifice at E12.0 (Figure 1A). RPCs in terminal S-phase at the time of injection retain BrdU label indefinitely, whereas, mitotic RPCs dilute BrdU in subsequent rounds of mitosis. The short window provided a baseline RPC mitotic index, with the long window chosen based on average RPC cell cycle length at this developmental stage (Alexiades and Cepko, 1996). Retinal sections were colabeled for BrdU, Ki67, and GFP (to mark the *Neurog2* lineage). We then quantified the percentage of GFP+ RPCs that remained mitotic (BrdU+Ki67+) versus those that exited the cell cycle (BrdU+Ki67-neg)(Chenn and Walsh, 2002; Kee et al., 2002; Pei et al., 2011). In the short window, there was a significant increase in mitotic RPCs in *Neurog2*$^{GFP/GFP}$ retinas, compared to *Neurog2*$^{GFP/+}$ or *Neurog2*$^{Ascl1KI/GFP}$ (Figure 1B). This increase was more pronounced in the longer time frame, but *Ascl1* provided full rescue during both labeling windows (Figures 2B-D). Interestingly, this outcome is not the same as ectopic expression of *Ascl1* in the *Atoh7* lineage. In that gene replacement mouse, both cell cycle exit and RGC differentiation were blocked, and the *Atoh7*$^{Ascl1KI/+}$ RPCs uniquely underwent extra rounds of mitosis (Hufnagel et al., 2013). Although the phenotypes of *Atoh7*$^{Ascl1KI/+}$and *Neurog2*$^{Ascl1KI/GFP}$ mice differed, in both situations ectopic *Ascl1* expression induced cell cycle progression.

Neurog2 regulation of RGC genesis

We next wished to correlate the window labeling findings with the progress of RGC differentiation. The RGC markers Pou4f and Isl1 had abnormal expression patterns in *Neurog2*$^{GFP/GFP}$ mutants, which were restored in *Neurog2*$^{Asc11KI/GFP}$ eyes (Hufnagel et al., 2010). However, these outcomes were not quantified. Using specific pan-Pou4f or Isl1 antibodies, we labeled E12.5 retinal sections, along with anti-GFP (Figures 2A-F), to determine the percentages of marker+GFP+ per total GFP+ cells (Figures 2G,H). Overall, we noted a reduction of Pou4f+ (8%) or Isl1+ (9%) cells in *Neurog2*$^{GFP/GFP}$ retinas, compared to *Neurog2*$^{GFP/+}$. There was also a rebound of Pou4f+ (3%) or Isl1+ (6%) cells in *Neurog2*$^{Ascl11KI/GFP}$ eyes, as compared to mutants. These shifts in nascent RGCs complemented the increased mitotic index found in *Neurog2*$^{GFP/GFP}$ eyes (4%) and its return to a nearly wild type rate in *Neurog2*$^{Ascl11KI/GFP}$ eyes (4%)(Figure 1B, short window). Thus, we concluded that *Neurog2* normally regulates both the terminal cell cycle exit and differentiation of early RGC neurons.

Genes expressed downstream of *Neurog2*

To generate an unbiased view of gene expression during the initial wave of neurogenesis, we compared the retinal transcriptomes of E12.5 *Neurog2*$^{GFP/+}$, *Neurog2*$^{GFP/GFP}$ and *Neurog2*$^{Ascl11KI/GFP}$ embryos. Because *Neurog2* heterozygotes are phenotypically

indistinguishable from wild type (Hufnagel et al., 2010), we took advantage of the live reporter in *Neurog2*$^{GFP/+}$, *Neurog2*$^{GFP/GFP}$ and *Neurog2*$^{Ascl1KI/GFP}$ to isolate GFP+ RPCs by flow cytometry, using the 7AAD dye to gate out any dying cells (Figure 3A). An average of 22,000 GFP+7AAD- RPCs were used for total RNA isolations from *Neurog2*$^{GFP/+}$ (n=14), *Neurog2*$^{GFP/GFP}$ (n=6), and *Neurog2*$^{Ascl1KI/GFP}$ (n=14) embryos (see Experimental Procedures for details). The resulting cDNA libraries then underwent Next-Gen sequencing. We used the Galaxy bioinformatics platform (www.galaxy.org) to analyze the resulting datasets (n = 3 biologic replicates/genotype). First we compared *Neurog2*$^{GFP/+}$ and *Neurog2*$^{GFP/GFP}$ transcriptomes, and then we compared the *Neurog2*$^{GFP/GFP}$ and *Neurog2*$^{Ascl1KI/GFP}$ transcriptomes (Figures 3,4). Genes whose transcript levels significantly differed ($q \leq 0.05$) were classified further by ontology, using the PANTHER program (www.geneontology.org). Those biologic processes with statistically valid changes in fold enrichment ($p \leq 0.05$) were then graphed relative to one another (Figures 3B, C). Groups associated with neurogenesis, neuronal differentiation and axon guidance were most highly downregulated in *Neurog2*$^{GFP/GFP}$ retinal cells, whereas smaller groups of genes regulating differentiation, or acting during morphogenesis were upregulated (Figure 3B). Remarkably, just two ontologic groups, neurogenesis and generation of neurons, were upregulated in *Neurog2*$^{Ascl1KI/GFP}$ eyes, with none of the groups listed in Figure 3B undergoing significant downregulation (Figure 3C).

As a proof of principle, we expected to see the absence of *Neurog2* transcripts in the *Neurog2*$^{GFP/GFP}$ and *Neurog2*$^{Ascl1KI/GFP}$ transcriptomes. Instead, the *Neurog2* RPKM values for both genotypes were higher than for heterozygotes (Figure 4). To explain this puzzling result, we visualized the distribution of the sequence reads at the *Neurog2* locus for all three genotypes, using the IGV program (Figure 5A). The *Neurog2* gene has two exons and one intron, with the open reading frame (ORF) located in the second exon (Gradwohl et al., 1996; Sommer et al., 1996; Fode et al., 1998). In both gene replacement strategies, *Neurog2* protein coding sequences were swapped out for either a GFP or *Ascl1* cDNA, thereby creating functionally null alleles that retained *Neurog2* 5′ and 3′ UTR sequences (Fode et al., 2000; Seibt et al., 2003). Our aligned sequence reads highlighted a bias among all three genotypes for the *Neurog2* UTRs. However, for both mutant alleles no sequence reads mapped to the ORF (Figure 5A). To independently verify this outcome, we performed real-time PCR using total RNA templates from E12.5 littermate GFP-sorted cells not used for the RNA libraries (Figure 5B). Direct comparison of the RQ values for Exon1 versus Exon2 ORF amplicons demonstrated significantly elevated Exon1 transcript expression in *Neurog2*$^{GFP/GFP}$ and *Neurog2*$^{Ascl1KI/GFP}$ retinas yet, undetectable levels of the Exon2 ORF (Figure 5B). We conclude that both mutant alleles are *Neurog2* nulls in the embryonic retina. Furthermore, biased distributions of *Neurog2* sequence reads containing 5′ and 3′ UTR segments obscured the lack of those for the protein-coding ORF.

Another gene predicted to be highly downregulated in *Neurog2* mutants was *Atoh7*, given that it is a direct transcriptional target (Skowronska-Krawczyk et al., 2009). However, only a small, −0.4X fold reduction was found (Figure 4; p=0.01). We attributed this to the developmental age of the starting material (E12.5). *Atoh7* expression levels were presumably even lower at the initiation of retinal neurogenesis (E11-E11.5), but in mutant cells isolated for sequencing, *Atoh7* transcription had probably begun to recover (Hufnagel

et al., 2010). So, we independently validated a significant downregulation of *Atoh7* mRNA in *Neurog2*$^{GFP/GFP}$ eyes by qPCR (Figure 6). Other bHLH factors also participate in aspects of RGC genesis, and subsets of *Atoh7*-lineage cells coexpress *Neurod1* and/or *Neurod4*/*Math3* (Mao et al., 2008; Mao et al., 2013). Interestingly, the substitution of either gene into the *Atoh7* locus rescued RGC genesis (Mao et al., 2008; Mao et al., 2013). Yet another bHLH factor, *Olig2*, is expressed broadly by RPCs, although functions related to RGC neurogenesis have not been described (Nakamura et al., 2006; Shibasaki et al., 2007; Hafler et al., 2012). In other CNS tissues *Olig2* specifies oligodendrocyte fates. All three factors, *Neurod1*, *Neurod4* and *Olig2*, were significantly downregulated in *Neurog2* mutants, with the latter two more severely affected (Figure 4).

Work by multiple labs has elucidated a transcription factor hierarchy acting during vertebrate RGC development (reviewed in Centanin and Wittbrodt, 2014; Stenkamp, 2015). Here *Atoh7* has been suggested to sit at a critical node, due to its early expression and phenotype, namely a total block of optic nerve formation, and reduced expression of many genes in the early RGC network. Immediately downstream of *Atoh7* are the factors *Pou4f2* and *Isl1*, which act synergistically to cement the RGC fate (Mu et al., 2008; Pan et al., 2008; Li et al., 2014; Wu et al., 2015). Additional relevant RGC factors are *Pou4f1,3*, *Isl2*, *Onecut1,2,3*, *Myt1* and *Ebf1,2,3*, which drive particular terminal differentiation processes, axonogenesis, and/or specify functional subclasses of RGCs (Xiang et al., 1995; Erkman et al., 1996; Gan et al., 1999; Mu et al., 2008; Jin et al., 2010; Wu et al., 2012; Shi et al., 2013). Thus, it was not unexpected to find a highly significant reduction in transcript levels for *Pou4f1*, *Pou4f2*, *Onecut2*, *Onecut3* and *Ebf3* in *Neurog2* mutants (Figures 4,6). Although downregulation of this entire set of early RGC regulators might be predicted, the transient nature of the *Neurog2* mutant phenotype, and cross-regulation among subsets of downstream factors could effectively mask changes in particular genes. For example, while *Ebf1*, *Ebf2*, and *Ebf3* are all expressed by nascent RGCs, only *Ebf3* is a direct target of *Pou4f2*, and was the sole *Ebf* paralogue significantly downregulated here (Jin et al., 2010; Gao et al., 2014) (Figures 4,6). We also noted a significant loss of the RGC axon guidance molecule, *Dcc* (Figures 4,6)(Deiner et al., 1997; Livesey and Hunt, 1997). These data are consistent with *Neurog2* activity residing sitting at the top of the early RGC genetic hierarchy.

Ascl1 Rescue Transcriptome

Another overt goal was to use transcriptomics to investigate the underlying basis of *Ascl1* rescue of the wave of neurogenesis in *Neurog2* mutants. Both *Neurog2*$^{GFP/GFP}$ and *Neurog2*$^{Ascl1KI/GFP}$ genotypes lacked functional *Neurog2*, but also showed upregulated endogenous *Ascl1* (Figures 4–6). The specificity of the latter outcome was also validated by qPCR, using primers specific for an endogenous *Ascl* gene amplicon (Figure 6). Among the gene expression lists with highly significant level changes ($q \leq 0.05$), we asked if there was a subset both downregulated in *Neurog2* mutants and upregulated in the *Ascl1* rescue. By these criteria we found just three genes with known roles in developmental neurobiology: *Neurod4*, *Pou4f2* and *Onecut2* (gray shading in Figure 4). We further confirmed these outcomes by qPCR, as well as verified expression level changes for other factors with less robust, but potentially meaningful alterations ($p \leq 0.05$)(Figures 4,6). We also noted four bHLH factors, *Atoh7*, *Neurod1*, *Neurod4* and *Olig2*, were each significantly increased in the

Neurog2$^{Ascl11KI/GFP}$ GFP lineage, although none were restored to the level of *Neurog2* heterozygotes (Figure 6). The simultaneous upregulation of four bHLH factors was quite striking, particularly when combined with the upregulation of *Pou4f2, Isl1* and *Onecut2* (Figure 6). Intriguingly, *Notch3* and *Hes5* levels were significantly altered in the *Neurog2*$^{GFP/GFP}$ versus *Neurog2*$^{Ascl11KI/GFP}$ transcriptomes (Figure 4), but only the changes in *Hes5* mRNA levels could be validated in a real-time PCR assay (Figure 6). Overall, we conclude that the loss of *Neurog2* stalls retinal neurogenesis, thereby stimulating upregulation of *Ascl1* to rescue RGC genesis, within a lineage where it is otherwise not normally active.

Discussion

Retinal neurogenesis is a dynamic process that requires the coordination of multiple cellular activities. One intrinsic, temporal regulator of neurogenesis is the proneural bHLH transcription factor *Neurog2* (Hufnagel et al., 2010). Here we demonstrate that *Neurog2* simultaneously regulates RPC cell cycle exit and early RGC differentiation. Transcriptomic analyses confirmed that although *Neurog2* activity is required for *Atoh7* expression, it also impacted a broader transcription factor network underlying RGC development. We also found that ectopic *Ascl1* drove this same network to a sufficient threshold that correlates with a rescue of RGC development.

Neurog2 regulation of cell cycle exit, and its rescue by *Ascl1*

Neurog2-mutant RPCs do not exit mitosis appropriately, relative to controls. This is consistent with *Neurog2* promotion of cell cycle exit in the spinal cord and neuronal culture, where it stabilizes the cyclin-dependent kinase inhibitor *Cdkn1b*/*p27*^{kip1} (Farah et al., 2000; Nguyen et al., 2006). By examining retinal cell cycle length via window labeling, we found an abnormal accumulation of mitotic RPCs in *Neurog2* mutants. We interpret this as a delay in cell cycle exit, since the proportion of S-phase RPCs is unaffected in E12.5 *Neurog2*$^{GFP/GFP}$ retinas (Hufnagel et al., 2010). We further propose that without *Neurog2*, RPCs accumulate at the G_1/G_0 checkpoint. *Neurog2* regulation of *Cdkn1b* in other developmental contexts make it an appealing molecule to be affected here, which could also explain the delay in retinal neurogenesis. However, no significant changes in *Cdkn1b* mRNA levels were found in *Neurog2*$^{GFP/GFP}$ versus *Neurog2*$^{GFP/+}$ transcriptomes. Nonetheless, loss of *Neurog2* might affect some other type of *Cdkn1b* regulation in the retina, and/or occur indirectly via *Atoh7*, since Cdkn1b+ cells are reduced in *Atoh7* mutant retinas (Le et al., 2006). Regardless of which gene controls *Cdkn1b* expression, the regulation presumably occurs post-transcriptionally. It would be interesting to explore these mechanisms in the future, by using *Cdkn1b* phosphorylation site-specific mutations, to test for temporal retinal neurogenesis phenotypes (Besson et al., 2006).

The mechanism by which *Ascl1* misexpression rescued the cell cycle phenotype of *Neurog2* mutant RPCs unfortunately remains unresolved. Throughout the nervous system, *Ascl1* was originally thought to promote cell cycle exit and neuronal differentiation (Ahmad et al., 1998; Cai et al., 2000; Tomita et al., 2000; Farah and Easter, 2005). Yet, genomic profiling studies in the brain demonstrated that *Ascl1* can activate the expression of cell cycle

progression genes, including canonical cell cycle regulators and oncogenic transcription factors (Castro et al., 2011). Although, we overtly searched for upregulated expression in these gene families, within the *Neurog2*$^{Ascl1KI/GFP}$ dataset, no such candidates were identified further evaluation. This would suggest that transcriptomic profiling to identify genes affected in temporal mutants may require tighter control of developmental time than is technically feasible during mouse embryogenesis.

Atoh7 as a direct downstream target gene for *Neurog2*

A key initiation step for retinal neurogenesis is *Neurog2* direct activation of *Atoh7* expression (Skowronska-Krawczyk et al., 2009). Lineage tracing and protein colocalization experiments show that in the embryonic retina, virtually all *Atoh7*^{LacZ} cells are also *Neurog2*+, but not the reverse situation (Hufnagel et al., 2010; Miesfeld et al., 2018). Thus, at any given point, the *Neurog2* lineage should include more RPCs, than the *Atoh7* lineage. Additionally, *Neurog2* and *Atoh7* are expressed during distinct cell cycle phases, with *Neurog2* largely found in mitotic cells, and *Atoh7* predominantly present in post-mitotic RPCs (Brown et al., 1998; Yang et al., 2003; Le et al., 2006; Ma and Wang, 2006; Brzezinski et al., 2012; Miesfeld et al., 2018). Together this suggests that a subset of *Neurog2*+ RPCs transit into *Atoh7*+ cells, complete cell cycle exit and differentiate. The *Atoh7* mRNA expression domain was clearly smaller in E11.5 *Neurog2* mutant retinas versus controls (Hufnagel et al., 2010), implying there would be a significant loss of *Atoh7* mRNA levels in mutant eyes. But, this was not the case for the *Neurog2* mutant transcriptome dataset, although we did find a significant loss by qPCR. These differing outcomes might be attributed to variability in the precise age of the samples collected for each assay. Another confounding variable could be a more limited sequencing efficiency at the *Atoh7* locus, due to high guanine-cytosine (GC) content. RNA-seq efficiency is reduced if GC content is either too high or too low (Risso et al., 2011; Zheng et al., 2011; Hansen et al., 2012; Filloux et al., 2014). The 5′ end of the *Atoh7* transcript contains a 185 nucleotide stretch with ≥85% GC content (Prasov et al., 2010), which could introduce a negative bias for sequence read-depth.

How does *Ascl1* “rescue” the *Neurog2* temporal phenotype?

In the developing mouse retina, *Ascl1* expression initiates about two days later than *Neurog2*, with its activity required for bipolar interneuron development and suppression of Müller glia (Jasoni and Reh, 1996; Tomita et al., 1996; Tomita et al., 2000; Brzezinski et al., 2011). Interestingly, the *Ascl1* lineage includes all major retinal cell classes, except for RGCs, and the loss of *Ascl1* does not impact RGC differentiation. Yet, one subset of Ascl1+ RPCs normally gives rise to *Atoh7*-expressing cells (Brzezinski et al., 2011). It is possible that in the *Neurog2* mutant lineage ectopic Ascl1 could directly activate *Atoh7* transcription, given the multiple E-box binding sites (CANNTG) in conserved *Atoh7* regulatory DNA (Murre et al., 1989; Hutcheson et al., 2005; Hufnagel et al., 2007; Skowronska-Krawczyk et al., 2009). The binding specificity between bHLH factors largely relies on variations in the central NN nucleotides, but in particular contexts sequences immediately surrounding the E-box are also influential (Powell et al., 2004; Seo et al., 2007; Gohlke et al., 2008; Gordan et al., 2013). In general, Ascl1 has high affinity for CAGCTG consensus sequences, whereas Neurog2 binds to CAGATC sequences (McNeill et al., 2012; Borromeo et al., 2014).

Alternatively, we propose that rather than inappropriate binding of ectopic Ascl1 to a preferred *Neurog2* consensus site, *Atoh7* transcription was prematurely stimulated via the same indirect regulatory mechanism normally employed within the endogenous *Ascl1* lineage (Brzezinski et al., 2011). Thus, the recovery of key genes in the RGC network in the *Neurog2*$^{Ascl1KI/GFP}$ dataset could be attributed to Ascl1 stimulation of *Atoh7* expression, which in turn activated the other genes. However simultaneous upregulation of four bHLH factors (along with *Pou4f2*, *Isl1* and *Onecut2*) suggests that ectopic Ascl1 induced the transcription of multiple genes. *Ascl1* was previously shown to control genetic cascades, which give rise to particular neuronal fates in the brain, and maintain the right size RPC pool for the late, postnatal retinal fates (Jasoni and Reh, 1996; Tomita et al., 1996; Tomita et al., 2000; Castro et al., 2011). *Ascl1* activity is also critical during retinal regeneration in multiple organisms (Wilken and Reh, 2016; Jorstad et al., 2017), and more recently implicated in mechanisms of tumorigenesis (Ma et al., 2017; Park et al., 2017). Thus, much more work is needed to tease apart the mode by which this factor successfully rescued RGC neurogenesis in the absence of *Neurog2*. Did *Ascl1* behave 'normally' but in a new context to activate *Atoh7*, or by virtue of its interactions with chromatin remodeling proteins, rapidly stimulate the transcription of an array of genes, above the minimum threshold necessary for RGC development?

Finally, we propose that *Neurog2* also occupies the critical node for RGC development, by virtue of its activation of *Atoh7*, plus other early bHLH factors. This is consistent with the significant downregulation of *Pou4f1,2*, *Isl1*, *Onecut2*, and *Ebf3* in *Neurog2* mutants (Xiang et al., 1995; Erkman et al., 1996; Gan et al., 1999; Mu et al., 2008; Jin et al., 2010; Wu et al., 2012; Shi et al., 2013). Arguably many of these same genes act downstream of and require *Atoh7*, but *Ascl1* only substitutes for *Neurog2*, and not *Atoh7* (Hufnagel et al., 2010; Hufnagel et al., 2013; Gao et al., 2014). Given that each bHLH factor has a "salt-and-pepper" pattern throughout retinogenesis, it provokes the question of how many bHLH factors an individual RPC must express at distinct timepoints, and whether particular combinations are sufficient to provide robustness for producing an RGC neuron. Although static co-expression pattern comparisons for all relevant transcription factors will be informative, we advocate single cell genomics to gain the most accurate understanding of the complex and important question of which early factors drive RGC genesis.

Experimental Procedures

Animals

Two gene replacement allele mouse strains were used in this study: *Neurog2*^{GFP} (*Neurog2*^{tm4Fgu}) (Seibt et al., 2003) and Neurog2^{Ascl1KI} (*Neurog2*$^{tm3(Ascl1)Fgu}$) (Fode et al., 2000), both maintained on an ICR background. PCR genotyping was as previously described (Fode et al., 2000; Seibt et al., 2003). Embryonic age was determined through timed matings, with the date of the vaginal plug as E0.5. All mice were housed and cared for in accordance with the guidelines provided by the National Institutes of Health, Bethesda, Maryland, and the Association for Research in Vision and Ophthalmology, and conducted with approval and oversight from the CCHRF and UC Davis Institutional Animal Care and Use Committees.

Immunohistochemistry and Cell Quantification

Embryos were fixed in 4% paraformaldehyde/PBS for 40-50 minutes at 4°C, cryoprotected in 5% and 15% sucrose/PBS, embedded in TissueTek OCT, and 10μm cryosections immuno-labeled as in (Mastick and Andrews, 2001). Primary antibodies used were rat anti-BrdU (AbD Serotec, Cat#:OBT0030, 1:100), chick anti-GFP (Abcam, 1:1000, AB13970), rabbit anti-Ki67 (Vector Labs, 1:1000, VP-K451), and rabbit anti-PH3 (Millipore-Sigma, 1:200, 06-570), goat anti-Pou4f (Santa Cruz 1:50, sc-6026), mouse anti-Isl1 IgG_{2B} (DSHB, 1:50, AB2314683). Secondary antibodies were conjugated to Alexa Fluor488 or Alexa Fluor594 (Invitrogen/Life Science, Grand Island, NY 1:500); or biotinylated (1:500) and sequentially labeled with streptavidin AMCA350 (Jackson ImmunoResearch, West Grove, PA, 1:200). Nuclear staining was performed with DAPI (1:1000 dilution of 10 mg/ml solution, Sigma, Cat#:28718-90-3).

Microscopy was performed with either a Zeiss fluorescent microscope, Zeiss camera and Apotome deconvolution device or a Leica DM5500 microscope, equipped with a SPEII solid state confocal. Images were processed using Zeiss Axiovision (v6.0), Leica LASAF and/or Adobe Photoshop (CS4) software programs. All digital micrographs were equivalently adjusted for brightness, contrast and pseudocoloring. Pou4f+GFP+ or Isl1+GFP+ cells were quantified using the count tool in Adobe Photoshop, CS4 and one-way ANOVA, plus a Bonferroni post-hoc test used to determine p-values (GraphPad Prism software (v6)). In all experiments ≥ 3 individuals per genotype were analyzed, using at least 2 sections per individual. Equivalent anatomical depth in the retina was determined by proximity to the optic nerve.

Mitotic Window Labeling

BrdU was injected into pregnant dams (0.1 mg/g body weight of 10 mg/mL BrdU in 0.9 M NaCl) at either 1.5 or 18 hours prior to embryo harvest. For all analyses, ≥ 3 biologic replicate embryos per age and genotype were analyzed. Ten micron cryosections were labeled as in (Le et al., 2006) and BrdU+, Ki67+, and BrdU+Ki67+ populations quantified within the *Neurog2*^{GFP} lineage, using the Axiovision measurements module. The percentage of GFP+BrdU+Ki67+ per GFP+BrdU+ cells ± standard error of the mean (SEM) was calculated within a 100× field, and one-way ANOVA, plus Tukey post-hoc test used to determine p values (Instat Software, v3).

Flow cytometry and RNA preparations

Pairs of E12.5 GFP+ optic cups were dissected and dissociated into single cell suspensions using TrypLE Select (Invitrogen, 12563). The eBioscience 7-AAD viability marker (ThermoFisher, 1:250, 00-6993-50) was added to all samples, and GFP+7AAD-neg cells purified with a Becton Dickenson FACS-Aria machine. Total RNA was immediately extracted using the RNeasy micro kit (Qiagen, Cat No 74004), and stored at −80°C. All samples were submitted to the CCHMC Gene Expression for quality assessment using an Agilent Bioanalyzer. Three biologic replicates per genotype were selected for RNA-seq analyses, through a combination of matched somites counts, average total RNA concentration (≥1.97 ng/μl) and RIN score (≥8.7). The selected samples were then submitted for transcriptome analysis.

RNA-seq and qPCR analyses

Sequencing libraries were generated using the TruSeq RNA library kit (Illumina, RS-122-2001), and analyzed on the Illumina Hi-Seq 2000, using single-end 50-bp read specifications with a read depth of ≥25 million (Illumina, San Diego, CA). Following removal of primers and barcodes, sequence reads were aligned to the mm10 mouse genome assembly with the BWA and Bowtie programs. Aligned reads were analyzed for differentially expressed transcripts using the CuffDiff program in the Galaxy bioinformatics package (www.usegalaxy.org). Differentially expressed transcripts were initially evaluated with an adjusted p-value cutoff of $q \leq 0.05$. For some transcripts, significance was broadened to $p \leq 0.05$, with the requirement of validation. Transcripts were grouped by ontology using PANTHER (www.geneontology.org) and ranked by fold enrichment. The sequence reads (RPKM) for particular genes were visualized with the Integrative Genomics Viewer (IGV) browser (v. 2.3)(Robinson et al., 2011; Thorvaldsdottir et al., 2013). RNA-seq datasets (see Supplemental Tables) were deposited in NCBI Gene Expression Omnibus (Edgar et al., 2002) and assigned accession number GSE111666 (https://www.ncbi.nlm.nih.gov/geo/query/acc.cgi?acc=GSE111666).

Real-time PCR was performed by reverse transcribing E12.5 total retinal RNA into cDNA using Superscript III (ThermoFisher, 18080093) and performing qPCR with primer sets listed below, Fast Sybr Green Master Mix (Applied BioSystems, Cat#:4385614) and an Applied BioSystems StepOnePlus machine. Relative quantification (RQ) values were calculated using the $2^{-\Delta\Delta CT}$ method (Livak and Schmittgen, 2001) with GAPDH as endogenous control. Statistical significance was determined using IBM SPSS Statistics (v. 24), with an unpaired 2-sample T-Test and Welsh correction.

qPCR Primer Pairs

Gene	Primer 1	Primer 2
Ascl1	TTGAACTCTATGGCGGGTTC	CAAAGTCCATTCCCAGGAGA
Atoh7	ATCACCCCTACCTCCCTTTCC	CGAAGAGCCTCTGCCCATA
Dcc	CAAGCTGGCTTTTGTACTCTTCG	GAACTCCTCGGTCGGACTCT
Ebf3	TCACCCTCCCTTCAAACTGTA	GTTTCACTGCGGAGATGACAT
Hes5	AGTCCCAAGGAGAAAAACCGA	GCTGTGTTTCAGGTAGCTGAC
Gapdh	TGAAGGGGTCGTTGATGG	AAAATGGTGAAGGTCGGTGT
Isl1	TATCCAGGGGATGACAGGAAC	GCTGTTGGGTGTATCTGGGAG
Neurod1	ATGACCAAATCATACAGCGAGAG	TCTGCCTCGTGTTCCTCGT
Neurod4	AGCTGGTCACACCACAATCCT	GTTCCGAGCATTCCATAAGAGC
Neurog2 exon1	AAGCAGCTCGGCTTTAACT	GTGTGTGTCCGGGAATGT
Neurog2 exon2	AACTCCACGTCCCCATACAG	GAGGCGCATAACGATGCTTCT
Notch3	AAGCGTCTCCTGGATGCTG	GAATCTGGAAGACAGCCTGG
Olig2	TCCCCAGAACCCGATGATCTT	CGTGGACGAGGACGCAGTC
Onecut1	GGCAACGTGAGCGGTAGTTT	TTGCTGGGAGTTGTGAATGCT
Onecut2	AGAGGGTTCTATGCCGGTCT	GGGATTTCTTCTGCGAGTTG
Pou4f1	AGGCCTATTTTGCCGTACAA	CGTCTCACACCCTCCTCAGT

Gene	Primer 1	Primer 2
Pou4f2	ATGGTGGTGGTGGCTCTTAC	CGGAGAGCTTGTCTTCCAAC
Prdm1 Exon6	TGCTCACTACCCCAAGTTCC	TGGGATAAGCACCTCTTTGG
Prdm1 3′UTR	GAACCTGCTTTTCAAGTATGCTG	AGTGTAGACTTCACCGATGAGG
Tubb3	TAGACCCCAGCGGCAACTAT	GTTCCAGGTTCCAAGTCCACC

Supplementary Material

Refer to Web version on PubMed Central for supplementary material.

Acknowledgments

The authors thank Francois Guillemot for *Neurog2*$^{GFP/+}$ and *Neurog2*$^{Ascl1KI/+}$ mice; Maxime Mahe for sharing microdissection expertise and FAC-sorting protocols; Tina Liu for technical help; the CCHMC Flow Cytometry, Gene Expression, and DNA Sequencing Cores for their services and guidance. We also thank the UC Davis eye development group for critical feedback and discussions; Richard Lang for use of a Zeiss Apotome imaging system, Rebekah Karns (CCHMC) and Monica Britton (UC Davis) for guidance with bioinformatics analyses. This work was funded by Prevent Blindness Ohio–Young Female Investigator in Vision Research Fellowship Award to KM, NEI training grant T32 EY015387 to AK; and NIH/NEI R01 grant EY13612 to NLB.

This work was funded by Prevent Blindness Ohio–Young Female Investigator in Vision Research Fellowship Award to KM, NEI training grant T32 EY015387 to AK; and NIH/NEI R01 grant EY13612 to NLB.

References

Ahmad I, Acharya HR, Rogers JA, Shibata A, Smithgall TE, Dooley CM. The role of NeuroD as a differentiation factor in the mammalian retina. J Mol Neurosci. 1998; 11:165–178. [PubMed: 10096043]

Alexiades MR, Cepko C. Quantitative analysis of proliferation and cell cycle length during development of the rat retina. Dev Dyn. 1996; 205:293–307. [PubMed: 8850565]

Besson A, Gurian-West M, Chen X, Kelly-Spratt KS, Kemp CJ, Roberts JM. A pathway in quiescent cells that controls p27Kip1 stability, subcellular localization, and tumor suppression. Genes Dev. 2006; 20:47–64. [PubMed: 16391232]

Borromeo MD, Meredith DM, Castro DS, Chang JC, Tung KC, Guillemot F, Johnson JE. A transcription factor network specifying inhibitory versus excitatory neurons in the dorsal spinal cord. Development. 2014

Brown NL, Kanekar S, Vetter ML, Tucker PK, Gemza DL, Glaser T. Math5 encodes a murine basic helix-loop-helix transcription factor expressed during early stages of retinal neurogenesis. Development. 1998; 125:4821–4833. [PubMed: 9806930]

Brown NL, Patel S, Brzezinski J, Glaser T. Math5 is required for retinal ganglion cell and optic nerve formation. Development. 2001; 128:2497–2508. [PubMed: 11493566]

Brzezinski JAtKim EJ, Johnson JE, Reh TA. Ascl1 expression defines a subpopulation of lineage-restricted progenitors in the mammalian retina. Development. 2011; 138:3519–3531. [PubMed: 21771810]

Brzezinski JAtPrasov L, Glaser T. Math5 defines the ganglion cell competence state in a subpopulation of retinal progenitor cells exiting the cell cycle. Dev Biol. 2012; 365:395–413. [PubMed: 22445509]

Cai L, Morrow EM, Cepko CL. Misexpression of basic helix-loop-helix genes in the murine cerebral cortex affects cell fate choices and neuronal survival. Development. 2000; 127:3021–3030. [PubMed: 10862740]

Castro DS, Martynoga B, Parras C, Ramesh V, Pacary E, Johnston C, Drechsel D, Lebel-Potter M, Garcia LG, Hunt C, Dolle D, Bithell A, Ettwiller L, Buckley N, Guillemot F. A novel function of

the proneural factor Ascl1 in progenitor proliferation identified by genome-wide characterization of its targets. Genes Dev. 2011; 25:930–945. [PubMed: 21536733]

Centanin L, Wittbrodt J. Retinal neurogenesis. Development. 2014; 141:241–244. [PubMed: 24381194]

Chenn A, Walsh CA. Regulation of cerebral cortical size by control of cell cycle exit in neural precursors. Science. 2002; 297:365–369. [PubMed: 12130776]

Deiner MS, Kennedy TE, Fazeli A, Serafini T, Tessier-Lavigne M, Sretavan DW. Netrin-1 and DCC mediate axon guidance locally at the optic disc: loss of function leads to optic nerve hypoplasia. Neuron. 1997; 19:575–589. [PubMed: 9331350]

Erkman L, McEvilly RJ, Luo L, Ryan AK, Hooshmand F, O'Connell SM, Keithley EM, Rapaport DH, Ryan AF, Rosenfeld MG. Role of transcription factors Brn-3.1 and Brn-3.2 in auditory and visual system development. Nature. 1996; 381:603–606. [PubMed: 8637595]

Farah MH, Easter SS Jr. Cell birth and death in the mouse retinal ganglion cell layer. J Comp Neurol. 2005; 489:120–134. [PubMed: 15977166]

Farah MH, Olson JM, Sucic HB, Hume RI, Tapscott SJ, Turner DL. Generation of neurons by transient expression of neural bHLH proteins in mammalian cells. Development. 2000; 127:693–702. [PubMed: 10648228]

Feng L, Xie ZH, Ding Q, Xie X, Libby RT, Gan L. MATH5 controls the acquisition of multiple retinal cell fates. Mol Brain. 2010; 3:36. [PubMed: 21087508]

Filloux C, Meersseman C, Philippe R, Forestier L, Klopp C, Rocha D, Maftah A, Petit D. An integrative method to normalize RNA-Seq data. BMC Bioinformatics. 2014; 15:188. [PubMed: 24929920]

Fode C, Gradwohl G, Morin X, Dierich A, LeMeur M, Goridis C, Guillemot F. The bHLH protein NEUROGENIN 2 is a determination factor for epibranchial placode-derived sensory neurons. Neuron. 1998; 20:483–494. [PubMed: 9539123]

Fode C, Ma Q, Casarosa S, Ang SL, Anderson DJ, Guillemot F. A role for neural determination genes in specifying the dorsoventral identity of telencephalic neurons. Genes Dev. 2000; 14:67–80. [PubMed: 10640277]

Gan L, Wang SW, Huang Z, Klein WH. POU domain factor Brn-3b is essential for retinal ganglion cell differentiation and survival but not for initial cell fate specification. Dev Biol. 1999; 210:469–480. [PubMed: 10357904]

Gan L, Xiang M, Zhou L, Wagner DS, Klein WH, Nathans J. POU domain factor Brn-3b is required for the development of a large set of retinal ganglion cells. Proc Natl Acad Sci U S A. 1996; 93:3920–3925. [PubMed: 8632990]

Gao Z, Mao CA, Pan P, Mu X, Klein WH. Transcriptome of Atoh7 retinal progenitor cells identifies new Atoh7-dependent regulatory genes for retinal ganglion cell formation. Dev Neurobiol. 2014

Gohlke JM, Armant O, Parham FM, Smith MV, Zimmer C, Castro DS, Nguyen L, Parker JS, Gradwohl G, Portier CJ, Guillemot F. Characterization of the proneural gene regulatory network during mouse telencephalon development. BMC Biol. 2008; 6:15. [PubMed: 18377642]

Gordan R, Shen N, Dror I, Zhou T, Horton J, Rohs R, Bulyk ML. Genomic regions flanking E-box binding sites influence DNA binding specificity of bHLH transcription factors through DNA shape. Cell Rep. 2013; 3:1093–1104. [PubMed: 23562153]

Gradwohl G, Fode C, Guillemot F. Restricted expression of a novel murine atonal-related bHLH protein in undifferentiated neural precursors. Dev Biol. 1996; 180:227–241. [PubMed: 8948587]

Hafler BP, Surzenko N, Beier KT, Punzo C, Trimarchi JM, Kong JH, Cepko CL. Transcription factor Olig2 defines subpopulations of retinal progenitor cells biased toward specific cell fates. Proc Natl Acad Sci U S A. 2012; 109:7882–7887. [PubMed: 22543161]

Hansen KD, Irizarry RA, Wu Z. Removing technical variability in RNA-seq data using conditional quantile normalization. Biostatistics. 2012; 13:204–216. [PubMed: 22285995]

Hu M, Easter SS. Retinal neurogenesis: the formation of the initial central patch of postmitotic cells. Dev Biol. 1999; 207:309–321. [PubMed: 10068465]

Hufnagel RB, Le TT, Riesenberg AL, Brown NL. Neurog2 controls the leading edge of neurogenesis in the mammalian retina. Dev Biol. 2010; 340:490–503. [PubMed: 20144606]

Hufnagel RB, Riesenberg AN, Quinn M, Brzezinski JAt, Glaser T, Brown NL. Heterochronic misexpression of Ascl1 in the Atoh7 retinal cell lineage blocks cell cycle exit. Mol Cell Neurosci. 2013; 54:108–120. [PubMed: 23481413]

Hufnagel RB, Riesenberg AN, Saul SM, Brown NL. Conserved regulation of Math5 and Math1 revealed by Math5-GFP transgenes. Mol Cell Neurosci. 2007; 36:435–448. [PubMed: 17900924]

Hutcheson DA, Hanson MI, Moore KB, Le TT, Brown NL, Vetter ML. bHLH-dependent and -independent modes of Ath5 gene regulation during retinal development. Development. 2005; 132:829–839. [PubMed: 15677728]

Jasoni CL, Reh TA. Temporal and spatial pattern of MASH-1 expression in the developing rat retina demonstrates progenitor cell heterogeneity. J Comp Neurol. 1996; 369:319–327. [PubMed: 8727003]

Jin K, Jiang H, Mo Z, Xiang M. Early B-cell factors are required for specifying multiple retinal cell types and subtypes from postmitotic precursors. J Neurosci. 2010; 30:11902–11916. [PubMed: 20826655]

Jorstad NL, Wilken MS, Grimes WN, Wohl SG, VandenBosch LS, Yoshimatsu T, Wong RO, Rieke F, Reh TA. Stimulation of functional neuronal regeneration from Muller glia in adult mice. Nature. 2017; 548:103–107. [PubMed: 28746305]

Kee N, Sivalingam S, Boonstra R, Wojtowicz JM. The utility of Ki-67 and BrdU as proliferative markers of adult neurogenesis. J Neurosci Methods. 2002; 115:97–105. [PubMed: 11897369]

Le TT, Wroblewski E, Patel S, Riesenberg AN, Brown NL. Math5 is required for both early retinal neuron differentiation and cell cycle progression. Dev Biol. 2006; 295:764–778. [PubMed: 16690048]

Li R, Wu F, Ruonala R, Sapkota D, Hu Z, Mu X. Isl1 and Pou4f2 form a complex to regulate target genes in developing retinal ganglion cells. PLoS One. 2014; 9:e92105. [PubMed: 24643061]

Livak KJ, Schmittgen TD. Analysis of relative gene expression data using real-time quantitative PCR and the 2(-Delta Delta C(T)) Method. Methods. 2001; 25:402–408. [PubMed: 11846609]

Livesey FJ, Hunt SP. Netrin and netrin receptor expression in the embryonic mammalian nervous system suggests roles in retinal, striatal, nigral, and cerebellar development. Mol Cell Neurosci. 1997; 8:417–429. [PubMed: 9143559]

Ma H, Du X, Zhang S, Wang Q, Yin Y, Qiu X, Da P, Yue H, Wu H, Xu F. Achaete-scute complex homologue-1 promotes development of laryngocarcinoma via facilitating the epithelial-mesenchymal transformation. Tumour Biol. 2017; 39:1010428317705752. [PubMed: 28618959]

Ma W, Wang SZ. The final fates of neurogenin2-expressing cells include all major neuron types in the mouse retina. Mol Cell Neurosci. 2006; 31:463–469. [PubMed: 16364654]

Mao CA, Cho JH, Wang J, Gao Z, Pan P, Tsai WW, Frishman LJ, Klein WH. Reprogramming amacrine and photoreceptor progenitors into retinal ganglion cells by replacing Neurod1 with Atoh7. Development. 2013; 140:541–551. [PubMed: 23293286]

Mao CA, Wang SW, Pan P, Klein WH. Rewiring the retinal ganglion cell gene regulatory network: Neurod1 promotes retinal ganglion cell fate in the absence of Math5. Development. 2008; 135:3379–3388. [PubMed: 18787067]

Mastick GS, Andrews GL. Pax6 regulates the identity of embryonic diencephalic neurons. Mol Cell Neurosci. 2001; 17:190–207. [PubMed: 11161479]

McCabe KL, Gunther EC, Reh TA. The development of the pattern of retinal ganglion cells in the chick retina: mechanisms that control differentiation. Development. 1999; 126:5713–5724. [PubMed: 10572047]

McNeill B, Perez-Iratxeta C, Mazerolle C, Furimsky M, Mishina Y, Andrade-Navarro MA, Wallace VA. Comparative genomics identification of a novel set of temporally regulated hedgehog target genes in the retina. Mol Cell Neurosci. 2012; 49:333–340. [PubMed: 22281533]

Miesfeld JB, Glaser T, Brown NL. The dynamics of native Atoh7 protein expression during mouse retinal histogenesis, revealed with a new antibody. Gene Expr Patterns. 2018; 27:114–121. [PubMed: 29225067]

Mu X, Fu X, Beremand PD, Thomas TL, Klein WH. Gene regulation logic in retinal ganglion cell development: Isl1 defines a critical branch distinct from but overlapping with Pou4f2. Proc Natl Acad Sci U S A. 2008; 105:6942–6947. [PubMed: 18460603]

Murre C, McCaw PS, Vaessin H, Caudy M, Jan LY, Jan YN, Cabrera CV, Buskin JN, Hauschka SD, Lassar AB, et al. Interactions between heterologous helix-loop-helix proteins generate complexes that bind specifically to a common DNA sequence. Cell. 1989; 58:537–544. [PubMed: 2503252]

Nakamura K, Harada C, Namekata K, Harada T. Expression of olig2 in retinal progenitor cells. Neuroreport. 2006; 17:345–349. [PubMed: 16514356]

Nguyen L, Besson A, Heng JI, Schuurmans C, Teboul L, Parras C, Philpott A, Roberts JM, Guillemot F. p27kip1 independently promotes neuronal differentiation and migration in the cerebral cortex. Genes Dev. 2006; 20:1511–1524. [PubMed: 16705040]

Pan L, Deng M, Xie X, Gan L. ISL1 and BRN3B co-regulate the differentiation of murine retinal ganglion cells. Development. 2008; 135:1981–1990. [PubMed: 18434421]

Park NI, Guilhamon P, Desai K, McAdam RF, Langille E, O'Connor M, Lan X, Whetstone H, Coutinho FJ, Vanner RJ, Ling E, Prinos P, Lee L, Selvadurai H, Atwal G, Kushida M, Clarke ID, Voisin V, Cusimano MD, Bernstein M, Das S, Bader G, Arrowsmith CH, Angers S, Huang X, Lupien M, Dirks PB. ASCL1 Reorganizes Chromatin to Direct Neuronal Fate and Suppress Tumorigenicity of Glioblastoma Stem Cells. Cell Stem Cell. 2017; 21:209–224 e207. [PubMed: 28712938]

Pei Z, Wang B, Chen G, Nagao M, Nakafuku M, Campbell K. Homeobox genes Gsx1 and Gsx2 differentially regulate telencephalic progenitor maturation. Proc Natl Acad Sci U S A. 2011; 108:1675–1680. [PubMed: 21205889]

Powell LM, Zur Lage PI, Prentice DR, Senthinathan B, Jarman AP. The proneural proteins Atonal and Scute regulate neural target genes through different E-box binding sites. Mol Cell Biol. 2004; 24:9517–9526. [PubMed: 15485919]

Prada C, Puga J, Perez-Mendez L, Lopez, Ramirez G. Spatial and Temporal Patterns of Neurogenesis in the Chick Retina. Eur J Neurosci. 1991; 3:1187. [PubMed: 12106248]

Prasov L, Brown NL, Glaser T. A critical analysis of Atoh7 (Math5) mRNA splicing in the developing mouse retina. PLoS One. 2010; 5:e12315. [PubMed: 20808762]

Rapaport DH, Wong LL, Wood ED, Yasumura D, LaVail MM. Timing and topography of cell genesis in the rat retina. J Comp Neurol. 2004; 474:304–324. [PubMed: 15164429]

Repka AM, Adler R. Accurate determination of the time of cell birth using a sequential labeling technique with [3H]-thymidine and bromodeoxyuridine ("window labeling"). J Histochem Cytochem. 1992; 40:947–953. [PubMed: 1607643]

Riesenberg AN, Le TT, Willardsen MI, Blackburn DC, Vetter ML, Brown NL. Pax6 regulation of Math5 during mouse retinal neurogenesis. Genesis. 2009; 47:175–187. [PubMed: 19208436]

Risso D, Schwartz K, Sherlock G, Dudoit S. GC-content normalization for RNA-Seq data. BMC Bioinformatics. 2011; 12:480. [PubMed: 22177264]

Robinson JT, Thorvaldsdottir H, Winckler W, Guttman M, Lander ES, Getz G, Mesirov JP. Integrative genomics viewer. Nat Biotechnol. 2011; 29:24–26. [PubMed: 21221095]

Seibt J, Schuurmans C, Gradwhol G, Dehay C, Vanderhaeghen P, Guillemot F, Polleux F. Neurogenin2 specifies the connectivity of thalamic neurons by controlling axon responsiveness to intermediate target cues. Neuron. 2003; 39:439–452. [PubMed: 12895419]

Seo S, Lim JW, Yellajoshyula D, Chang LW, Kroll KL. Neurogenin and NeuroD direct transcriptional targets and their regulatory enhancers. EMBO J. 2007; 26:5093–5108. [PubMed: 18007592]

Shi M, Kumar SR, Motajo O, Kretschmer F, Mu X, Badea TC. Genetic interactions between Brn3 transcription factors in retinal ganglion cell type specification. PLoS One. 2013; 8:e76347. [PubMed: 24116103]

Shibasaki K, Takebayashi H, Ikenaka K, Feng L, Gan L. Expression of the basic helix-loop-factor Olig2 in the developing retina: Olig2 as a new marker for retinal progenitors and late-born cells. Gene Expr Patterns. 2007; 7:57–65. [PubMed: 16815098]

Sidman RL. Histogenesis of mouse retina studied with thymidine-H3. New York: Academic Press; 1961.

Skowronska-Krawczyk D, Chiodini F, Ebeling M, Alliod C, Kundzewicz A, Castro D, Ballivet M, Guillemot F, Matter-Sadzinski L, Matter JM. Conserved regulatory sequences in Atoh7 mediate non-conserved regulatory responses in retina ontogenesis. Development. 2009; 136:3767–3777. [PubMed: 19855019]

Sommer L, Ma Q, Anderson DJ. neurogenins, a novel family of atonal-related bHLH transcription factors, are putative mammalian neuronal determination genes that reveal progenitor cell heterogeneity in the developing CNS and PNS. Mol Cell Neurosci. 1996; 8:221–241. [PubMed: 9000438]

Stenkamp DL. Development of the Vertebrate Eye and Retina. Prog Mol Biol Transl Sci. 2015; 134:397–414. [PubMed: 26310167]

Thorvaldsdottir H, Robinson JT, Mesirov JP. Integrative Genomics Viewer (IGV): high-performance genomics data visualization and exploration. Brief Bioinform. 2013; 14:178–192. [PubMed: 22517427]

Tomita K, Moriyoshi K, Nakanishi S, Guillemot F, Kageyama R. Mammalian achaete-scute and atonal homologs regulate neuronal versus glial fate determination in the central nervous system. EMBO J. 2000; 19:5460–5472. [PubMed: 11032813]

Tomita K, Nakanishi S, Guillemot F, Kageyama R. Mash1 promotes neuronal differentiation in the retina. Genes Cells. 1996; 1:765–774. [PubMed: 9077445]

Turner DL, Cepko CL. A common progenitor for neurons and glia persists in rat retina late in development. Nature. 1987; 328:131–136. [PubMed: 3600789]

Turner DL, Snyder EY, Cepko CL. Lineage-independent determination of cell type in the embryonic mouse retina. Neuron. 1990; 4:833–845. [PubMed: 2163263]

Wang SW, Kim BS, Ding K, Wang H, Sun D, Johnson RL, Klein WH, Gan L. Requirement for math5 in the development of retinal ganglion cells. Genes Dev. 2001; 15:24–29. [PubMed: 11156601]

Wilken MS, Reh TA. Retinal regeneration in birds and mice. Curr Opin Genet Dev. 2016; 40:57–64. [PubMed: 27379897]

Wu F, Kaczynski TJ, Sethuramanujam S, Li R, Jain V, Slaughter M, Mu X. Two transcription factors, Pou4f2 and Isl1, are sufficient to specify the retinal ganglion cell fate. Proc Natl Acad Sci U S A. 2015; 112:E1559–1568. [PubMed: 25775587]

Wu F, Sapkota D, Li R, Mu X. Onecut 1 and Onecut 2 are potential regulators of mouse retinal development. J Comp Neurol. 2012; 520:952–969. [PubMed: 21830221]

Xiang M, Zhou L, Macke JP, Yoshioka T, Hendry SH, Eddy RL, Shows TB, Nathans J. The Brn-3 family of POU-domain factors: primary structure, binding specificity, and expression in subsets of retinal ganglion cells and somatosensory neurons. J Neurosci. 1995; 15:4762–4785. [PubMed: 7623109]

Yan RT, Ma WX, Wang SZ. neurogenin2 elicits the genesis of retinal neurons from cultures of nonneural cells. Proc Natl Acad Sci U S A. 2001; 98:15014–15019. [PubMed: 11752450]

Yang Z, Ding K, Pan L, Deng M, Gan L. Math5 determines the competence state of retinal ganglion cell progenitors. Dev Biol. 2003; 264:240–254. [PubMed: 14623245]

Young RW. Cell differentiation in the retina of the mouse. Anat Rec. 1985; 212:199–205. [PubMed: 3842042]

Zheng W, Chung LM, Zhao H. Bias detection and correction in RNA-Sequencing data. BMC Bioinformatics. 2011; 12:290. [PubMed: 21771300]

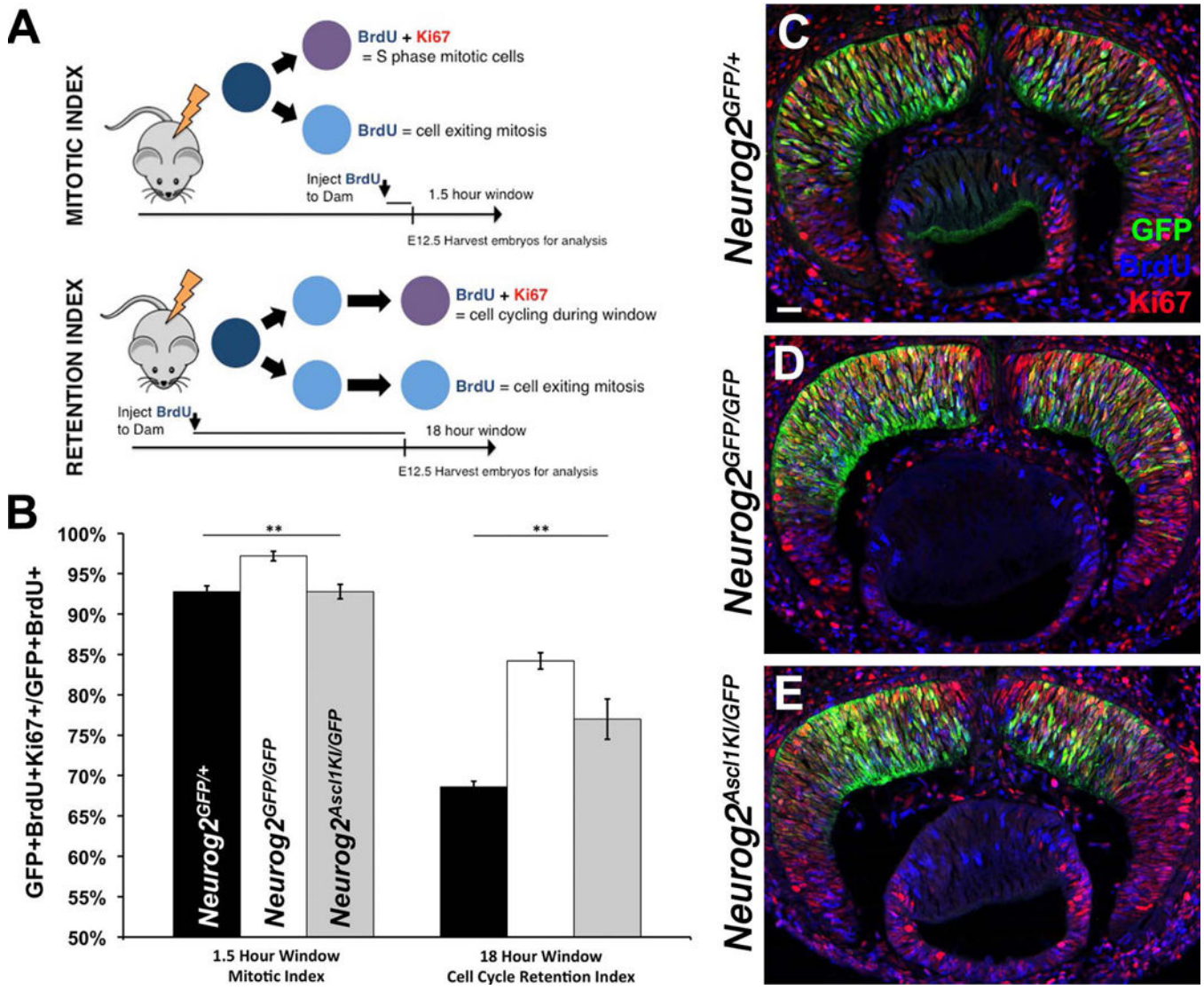

Figure 1. *Neurog2* is required for retinal progenitor cell cycle exit

A) Experimental strategy to label RPCs with BrdU for 1.5 or 18 hours prior to embryo harvest at E12.0. **B)** Percentages of *Neurog2* lineage cells (GFP+) in the cell cycle. There was a significant increase in mitotic RPCs in $Neurog2^{GFP/GFP}$ retinas, which was more apparent with a longer labeling window. *Ascl1* recombined into the *Neurog2* locus rescued this phenotype. **C-E)** Representative triple-labeled retinal images for $Neurog2^{GFP/+}$, $Neurog2^{GFP/GFP}$, and $Neurog2^{Ascl1KI/GFP}$ embryos after 18 hour BrdU labeling. A one-way ANOVA, plus Tukey post-hoc test was used to determine p-values. **$p \leq 0.01$; error bars = SEM; $n \geq 3$ embryos/genotype; apical is up; scale bar = 50μm.

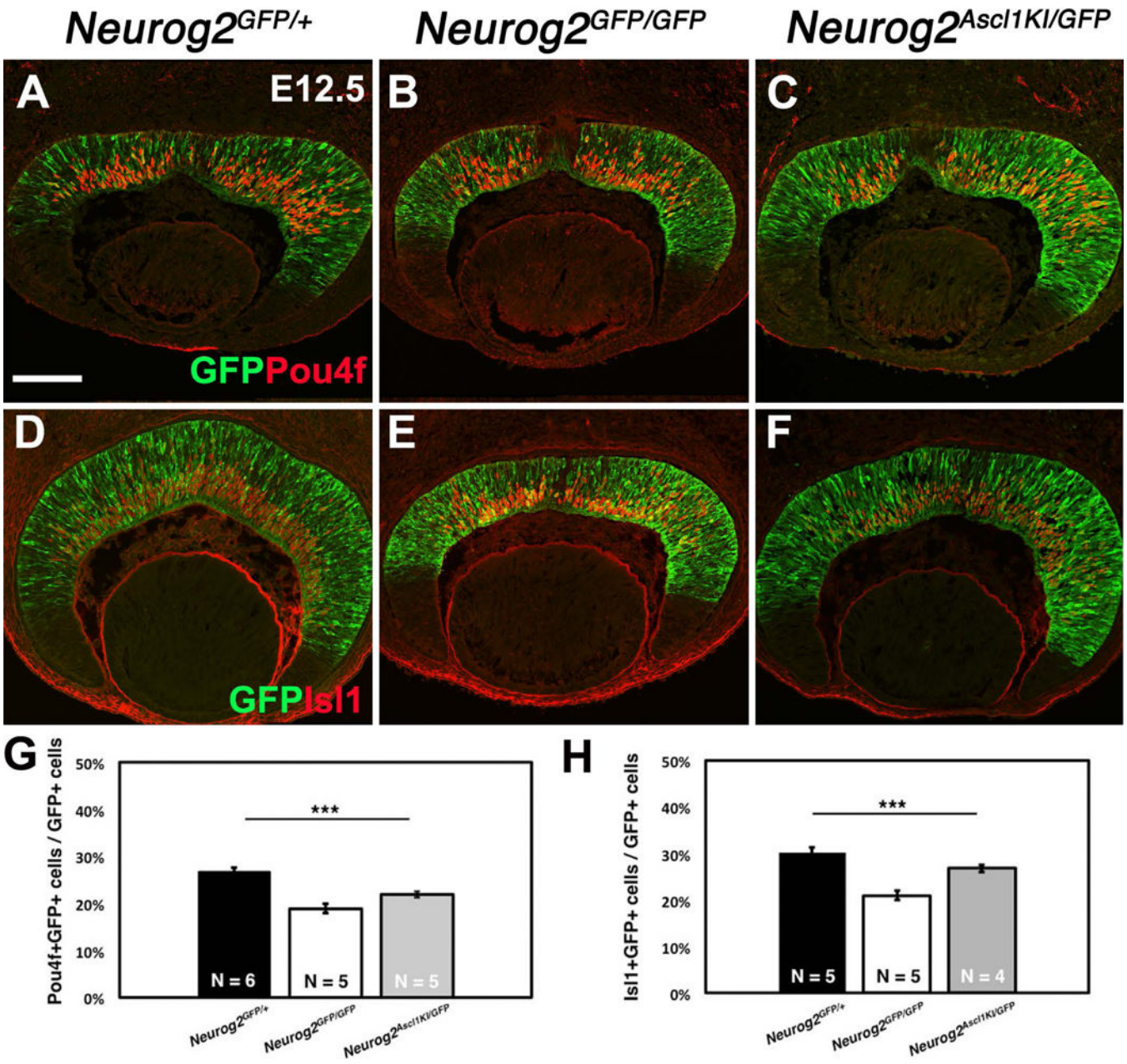

Figure 2. The impact of *Neurog2* loss on RGC differentiation

A-C,G) E12.5 Pou4f+ RGCs in the *Neurog2*^{GFP} lineage are significantly reduced in *Neurog2* mutants but rescued by *Ascl1* misexpression in the *Neurog2* locus. **D-F,H)** E12.5 Isl1+ cells (most of which are RGCs) are analogously reduced in *Neurog2* mutants and rescued by *Ascl1*. A one-way ANOVA, plus Bonferroni post-hoc test were used to determine p-values. ***p ≤ 0.001; error bars = SEM; apical retina is up; n ≥ 3 embryos/genotype; scale bar = 100μm.

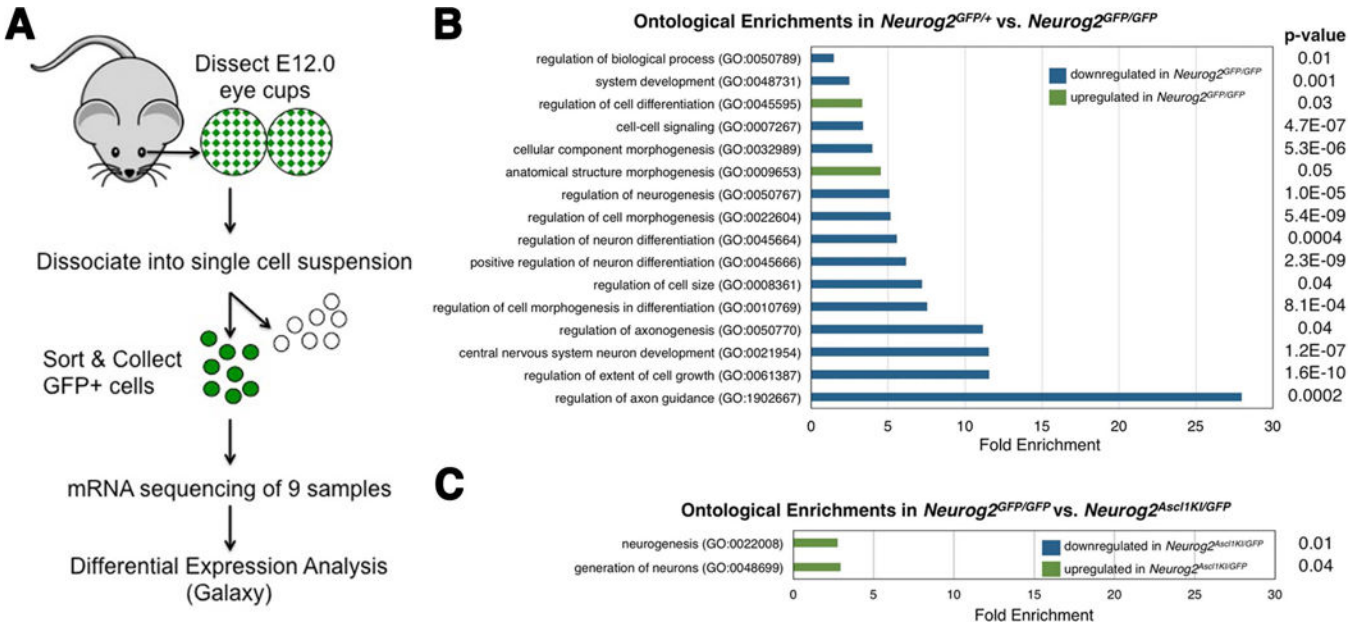

Figure 3. High-throughput analysis of transcriptional changes in E12.5 *Neurog2*-GFP+ RPCs among three genotypes

A) Work flow diagram of optic cup collection, dissociation and flow-sorting of GFP+;7-AAD-neg populations from *Neurog2*$^{GFP/+}$, *Neurog2*$^{GFP/GFP}$, and *Neurog2*$^{Ascl1KI/GFP}$ embryos, followed by RNA-seq analyses**. B)** Gene ontology analyses among the genotypes, with statistically significant functional groups ranked by fold enrichment. Blue bars indicate G0 categories with significant downregulated gene expression; green bars denote categories with significant upregulated expression.

Gene Name	GFP/+ RPKM Value	GFP/GFP RPKM Value	Ascl1KI/GFP RPKM Value	GFP/+ vs. GFP/GFP Log2 (Fold Change)	p-value	Adj. p-value	GFP/GFP vs. Ascl1KI/GFP Log2 (Fold Change)	p-value	Adj. p-value	Encoded protein, proposed function
Ascl1 **	7.4	14.9	15.7	1	5 X10^{-5}	0.01	0.11	NS	NS	Transcription factor, Neurogenesis
Neurog2 **	30.2	35.5	112.3	0.3	NS	NS	1.6	5X10^{-5}	0.01	Transcription factor, Neurogenesis
Atoh7 **	195.3	145	206	-0.4	0.01	NS	0.5	0.0009	NS	Transcription factor, RGC development
Pou4f1 **	7.5	3.1	3.8	-1.5	5 X10^{-5}	0.01	0.3	NS	NS	Transcription factor, RGC development
Pou4f2 **	53.1	30.5	70.9	-0.8	5X10^{-5}	0.01	1.2	5X10^{-5}	0.01	Transcription factor, RGC development
Isl1 **	16.3	12.8	24.1	-0.4	NS	NS	0.63	0.01	NS	Transcription factor, Neurogenesis
Onecut1	0.76	1.1	5.1	0.6	NS	NS	0.4	NS	NS	Transcription factor, Cell Fate Determination
Onecut2 **	16.6	7.7	25.3	-1	0.0002	0.04	0.7	5X10^{-5}	0.01	Transcription factor, Cell Fate Determination
Onecut3	3.8	1.2	1	-1.6	5X10^{-5}	0.01	-0.2	NS	NS	Transcription factor, Cell Fate Determination
Ebf3	28.9	11.6	18	-1.3	0.0001	0.02	0.6	NS	NS	Transcription factor, Differentiation
Olig2 **	4.6	2.5	2.8	-0.9	0.0003	0.04	0.2	NS	NS	Transcription factor, Neurogenesis/Gliogenesis
Neurod1 **	41.8	29	32.3	-0.5	0.02	NS	0.14	NS	NS	Transcription factor, Cell Differentiation
Neurod4 **	18.3	9.4	15.1	-1	5X10^{-5}	0.01	0.7	5X10^{-5}	0.01	Transcription factor, Neural Development
Notch3 **	5.4	5	8	-0.08	NS	NS	0.7	5X10^{-5}	0.01	Notch receptor, Signal Transduction
Hes5 **	64.1	42.3	21.3	-0.6	0.001	NS	-1	5X10^{-5}	0.01	Transcription factor, Signal Transduction
Hey1	61.4	47	51.2	-0.4	0.009	NS	0.14	NS	NS	Ttranscription factor, Signal Transduction
Dcc **	53.8	32.6	37.8	-0.7	5X10^{-5}	0.01	0.23	NS	NS	Transmembrane protein, Axon Guidance
Prdm1 #	17.8	10.7	11	-0.7	5X10^{-5}	0.01	0.05	NS	NS	Transcription factor, Differentiation
Prdm13	2.3	0.7	1.1	-1.7	5X10^{-5}	0.01	0.65	0.04	NS	Transcription factor, Differentiation
Acsl6	9.7	3.8	10.3	-1.3	0.0001	0.02	0.24	NS	NS	Acyl-CoA synthetase long-chain fam member 6
Camk2n1	24	13.9	22.9	-0.8	5X10^{-5}	0.01	0.7	5X10^{-5}	0.01	Calcium/calmodulin-dependent protein kinase II inhibitor 1
Cd59a	21.7	13.3	23.2	-0.7	0.0003	0.04	0.8	5X10^{-5}	0.01	Complement protein
Gje1	20.7	52	34	1.3	5X10^{-5}	0.01	-0.6	0.0003	0.04	Gap junction protein epsilon 1
Insm2	16.8	10.7	16	-0.6	0.0002	0.03	0.6	2.5 X10^{-5}	0.04	Insulinoma-associated protein
Nova2	12.7	6.1	9.9	-1	5X10^{-5}	0.01	0.7	5X10^{-5}	0.01	Neuro-oncological ventral antigen
Nsg2	16	7.6	11.8	-1.1	5X10^{-5}	0.01	0.7	0.0002	0.04	Neuron specific gene family member 2
Rab3c	2.6	1.3	2.2	-1	5X10^{-5}	0.01	0.7	0.0002	0.03	GTPase
Tmem60	42.4	74	29	0.8	5X10^{-5}	0.01	-1.3	5X10^{-5}	0.01	Transmembrane protein 60
Trappc6b	73	46	71	-0.7	5X10^{-5}	0.01	0.6	0.0002	0.03	Trafficking protein particle complex 6b

Figure 4. Retinal development genes displaying significant expression changes among E12.5 *Neurog2*$^{GFP/+}$, *Neurog2*$^{GFP/GFP}$ *Neurog2*$^{AscII1KI/GFP}$ cells

Two, selected alphabetical lists of genes with significant changes in gene expression. The first group are those known to act during early retinogenesis, the second group are largely active in the CNS. Columns 2-4 are reads per kilobase of transcript per million mapped reads (RPKM) values. The log-fold change between two different genotypes are listed in columns 5 and 8, followed by statistical significance in columns 6 and 9 = p-values; columns 7 and 10 = q-values. Some transcripts had significant q-values in one genotypic comparison, but not the other. Those genes validated by qPCR are denoted with ** or #. (# Prdm1 validation can be found in Kowalchuk et al 2018# Prdm1 validation can be found in Kowalchuk et al in press). Three genes in the top group (gray shading) were significantly downregulated in *Neurog2* mutants and upregulated by ectopic *Ascl1*.

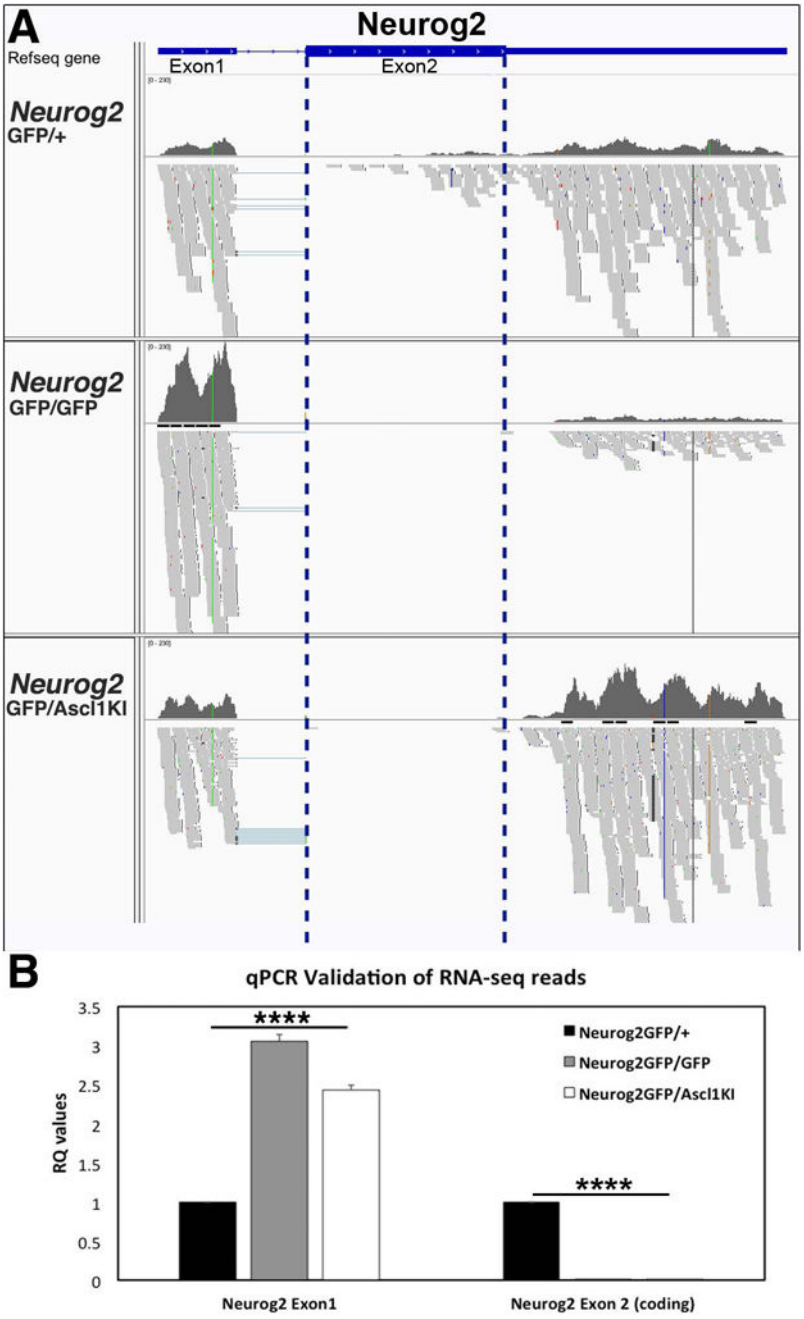

Figure 5. *Neurog2* RNA-seq transcription profiles for gene replacement mutations

IGV browser view of high-throughput sequences aligned to the *Neurog2* genomic locus (mm10). **A)** In all three genotypes, many reads mapped to 5′ or 3′ UTR. Blue dotted lines demarcate the ORF within Exon2 and better highlight the lack of sequence reads for both mutants. These alleles were made through precise replacement of *Neurog2* coding sequences with GFP or *Ascl1* cDNA, but retention of both endogenous UTRs (Fode et al., 2000; Seibt et al., 2003). **B)** Exon-specific qPCR using optic cup cDNA from E12.5 littermates of those used for RNA-seq libraries. Exon1 mRNA is elevated over control in both mutants, but both

mutants lack Exon2-ORF mRNA. n = 3 biologic replicates/genotype; **** $p \leq 0.0001$; error bars = SEM.

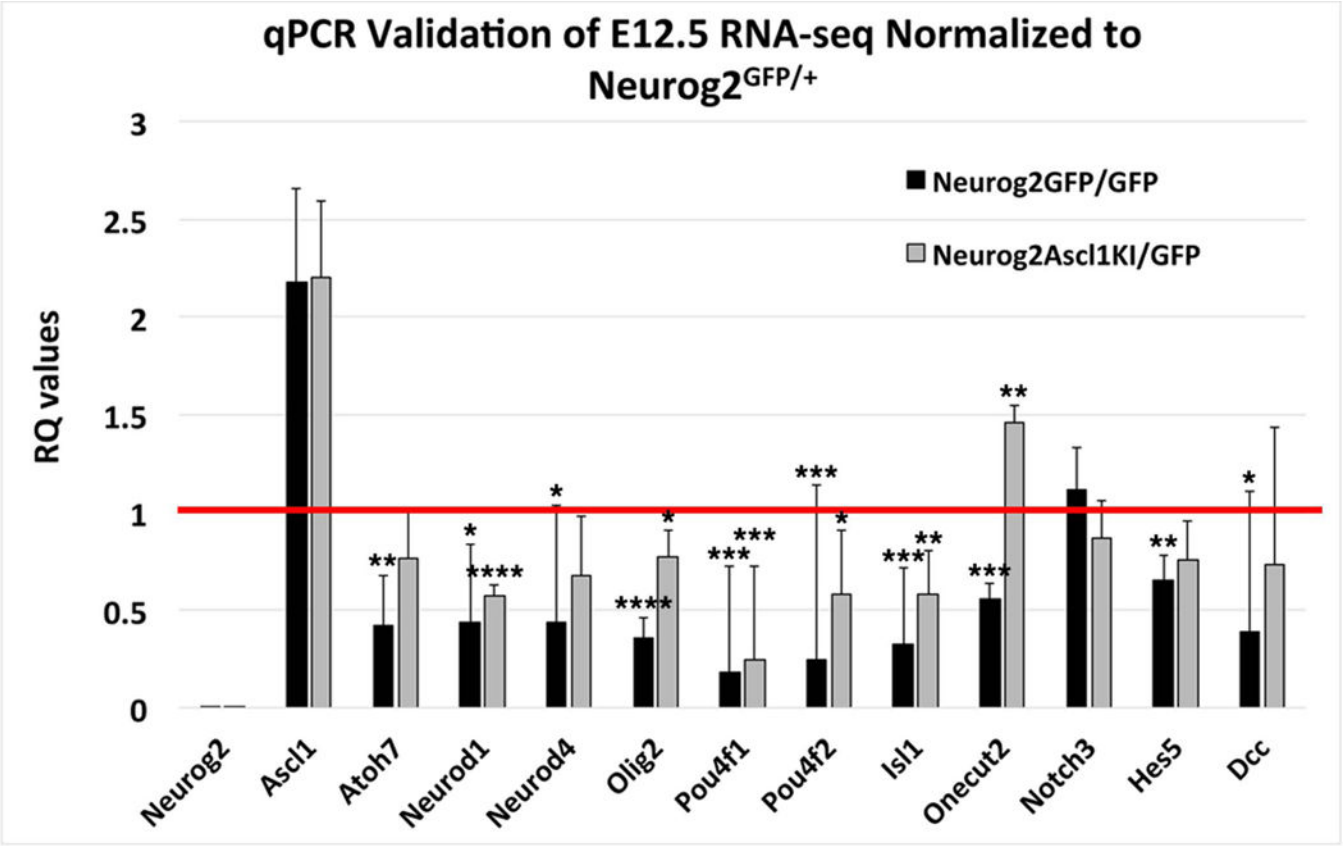

Figure 6. Validation of gene expression changes in a *Neurog2* allelic series

qPCR outcomes for thirteen genes with significant q and/or p-values among the transcriptomic datasets. Elevated *Ascl1* levels solely reflect endogenous transcripts, since one primer resides in *Ascl1* 3′UTR that is not present in this replacement allele. *Neurog2*$^{GFP/+}$ cell transcript levels were normalized to 1. The *Neurog2* Exon2-ORF data from Fig 5B was also included here for comparison. n = 3 biologic replicates/genotype; *p ≤ 0.05; **p ≤ 0.01; ***p ≤ 0.001; **** p ≤ 0.0001; error bars = SEM.